

***PR12-20-004 PRad-II: A New Upgraded High
Precision Measurement of the Proton Charge Radius***

Haiyan Gao

Duke University

for the PRad Collaboration

JLab PAC 48, August 2020

***Spokespersons: D. Dutta, H. Gao, A. Gasparian (contact), D. Higinbotham,
N. Liyanage, E. Pasyuk, C. Peng***



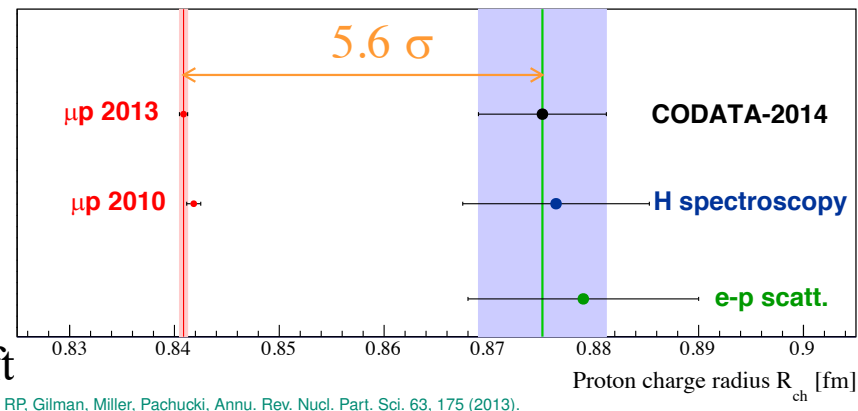
Outline

- Physics Motivation
- PRad experiment and the results
- Overview of PRad-II
- Proposed measurements and improvements
- Beam request and projected results
- Summary

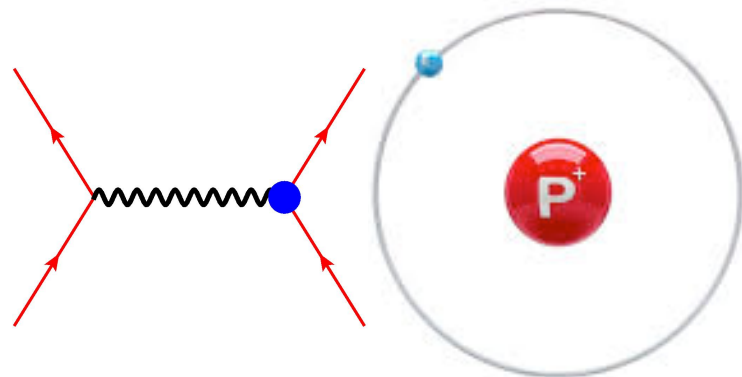


Proton Charge Radius

- QCD: still poorly understood in non-pQCD region
- Nucleon structure: active areas of research
- Proton charge radius:
 1. A fundamental quantity for proton
 2. Important for understanding how QCD works
 3. An important physics input to the bound state QED calculation, affects muonic H Lamb shift ($2S_{1/2} - 2P_{1/2}$) by as much as 2%
 1. Critical in determining Rydberg constant



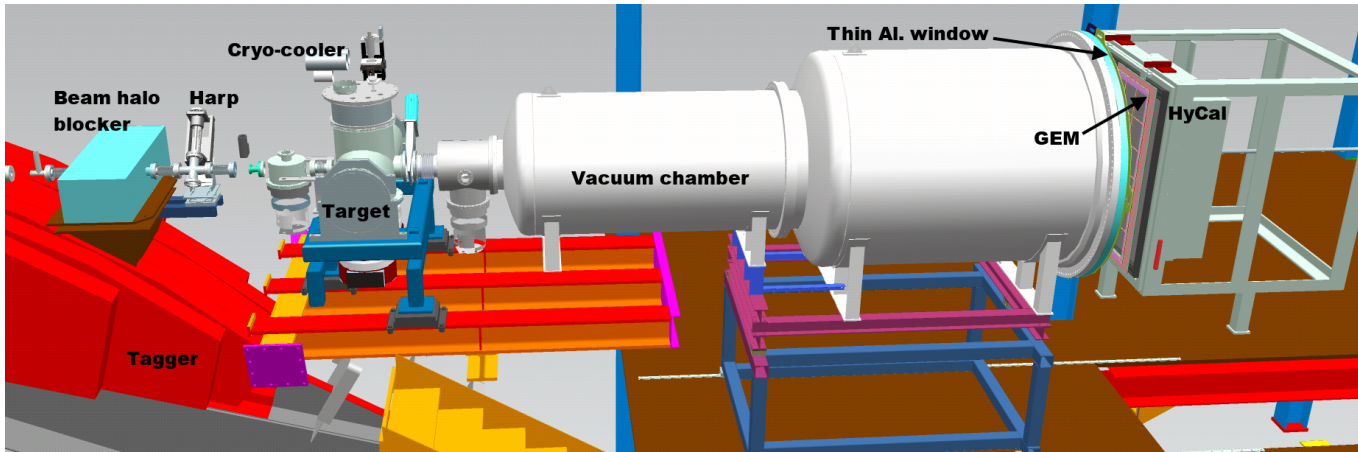
- Methods to measure the proton charge radius:
 1. Hydrogen spectroscopy (**atomic physics**)
 - Ordinary hydrogen
 - Muonic hydrogen
 2. Lepton-proton elastic scattering (**nuclear physics**)
 - ep elastic scattering (like PRad)
 - μp elastic scattering (like MUSE, COMPASS++/AMBER)



$$\sqrt{\langle r^2 \rangle} = \sqrt{-6 \frac{dG(q^2)}{dq^2} \Big|_{q^2=0}}$$

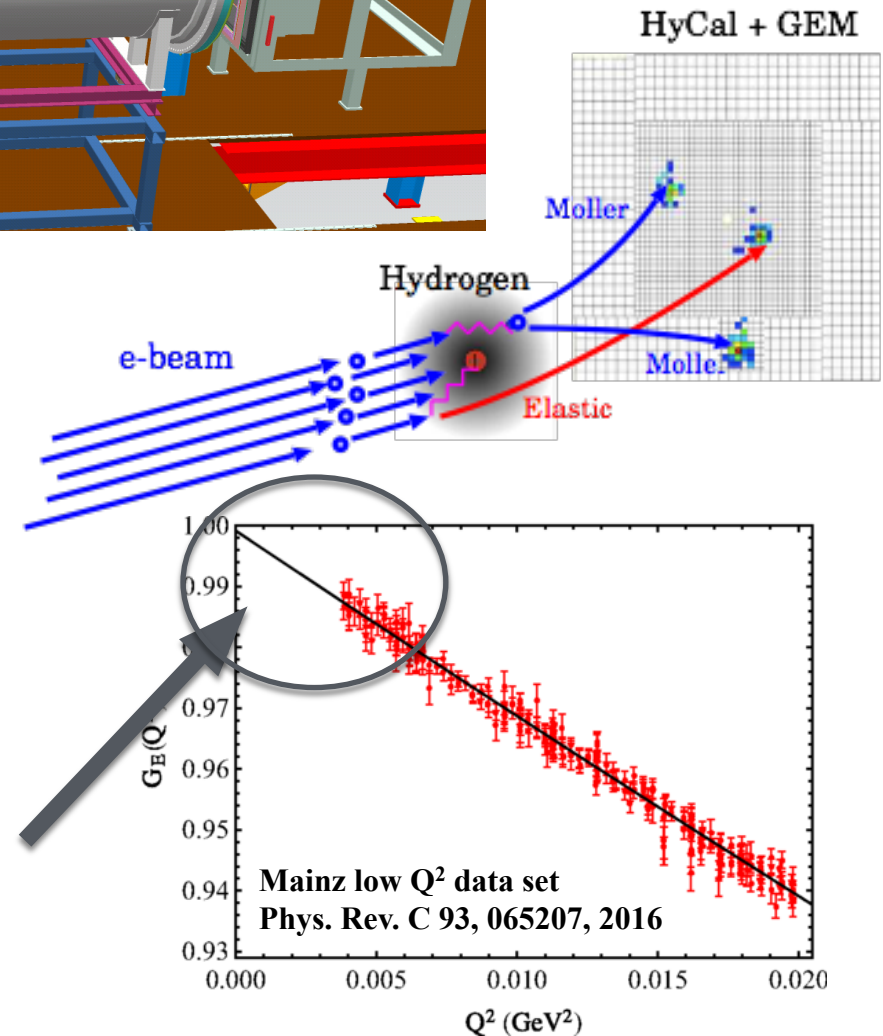
- Important point: the proton radius measured in lepton scattering is defined in the same way as in atomic spectroscopy (G.A. Miller, 2019)

PRad: an experiment to help solve the puzzle

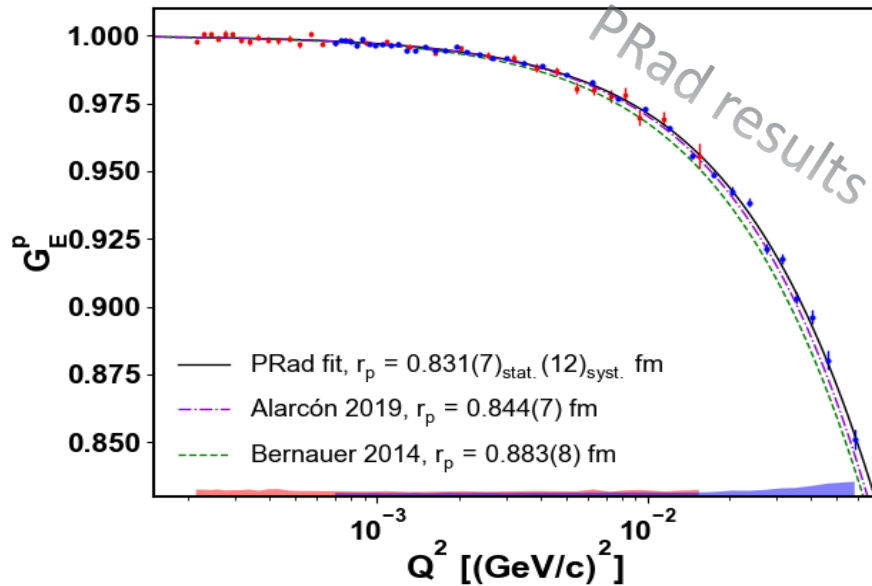


- High resolution, large acceptance, hybrid HyCal calorimeter (**PbWO₄** and **Pb-Glass**)
- Large-area GEM detector for better position measurement
- Windowless H₂ gas flow target
- Simultaneous detection of elastic and Moller electrons
- **Q² range of 2x10⁻⁴ – 0.06 GeV²**
- Vacuum chamber

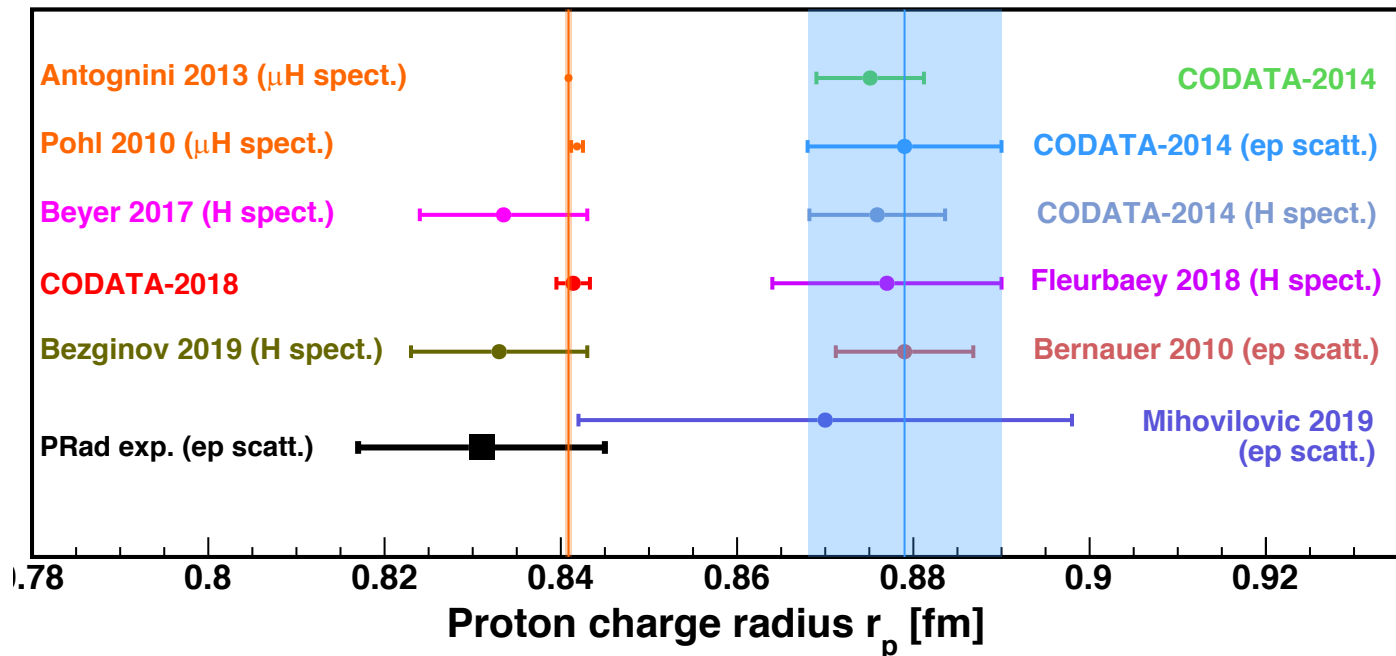
**Spokespersons: A. Gasparian (contact),
H. Gao, D. Dutta, M. Khandaker**



Results from PRad Experiment



- PRad result $r_p = 0.831 \pm 0.007$ (stat.) ± 0.012 (syst.) fm supports a smaller radius,
Xiong *et al.*, *Nature* 575, 147–150 (2019)
- PRad result included in the latest Particle Data Group
- CODATA released (online) revised 2018 value of r_p : 0.8414 ± 0.0019 fm (online in 2019)
- CODATA also shifted the value of the Rydberg constant
- New hydrogen Lamb Shift measurement also supports smaller radius, **Bezginov *et al.*, *Science* 365, 1007-1012 (2019)**



Why PRad-II?



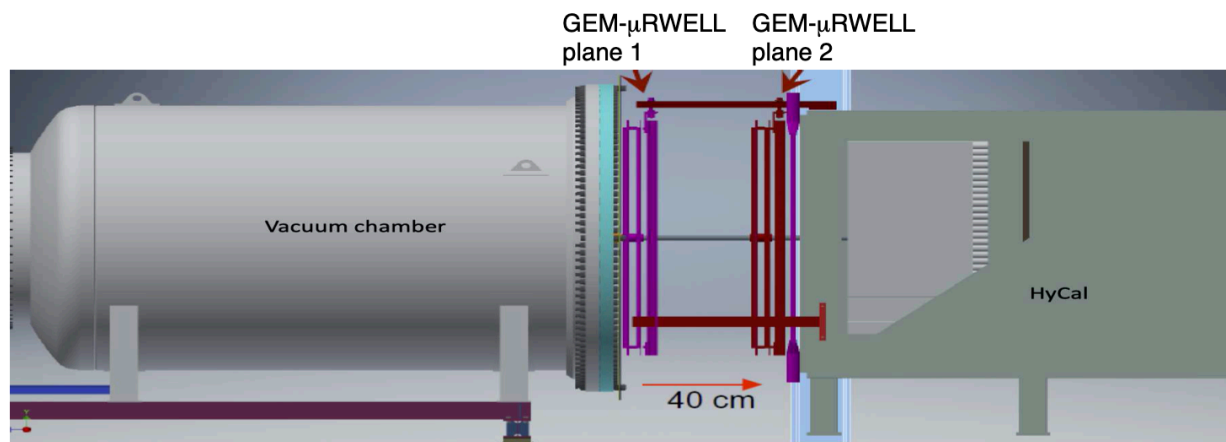
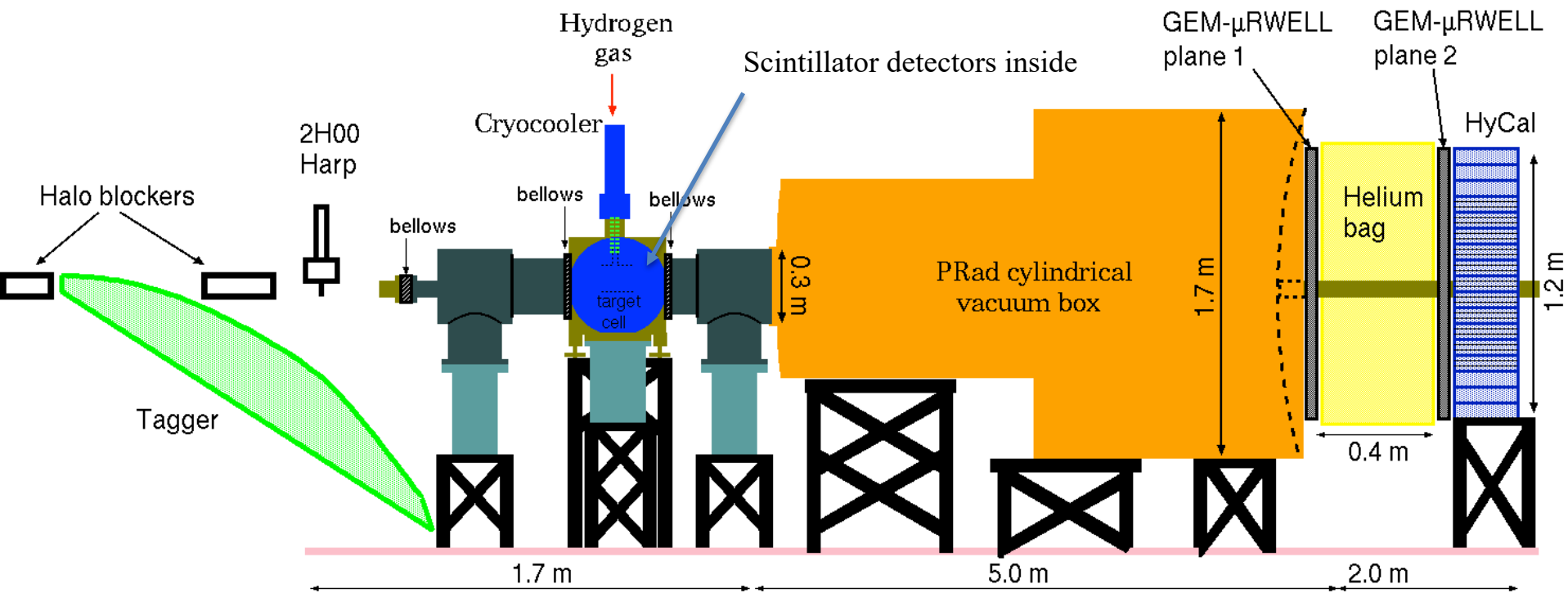
- PRad demonstrated the power of magnetic-spectrometer-free calorimetric method for proton charge radius measurement -- *but has not reached its ultimate precision*
- PRad – first electron scattering experiment measured a proton charge radius consistent with muonic results
- PRad proton electric form factor results show systematic difference from those of Mainz (2010) – *higher precision is demanded*
- Is there a possible difference between proton radius from electronic versus muonic system?
 - PRad and two recent hydrogen spectroscopic results show smaller central values than muonic value, albeit with larger experimental uncertainties – *calls for improved precision*
 - Discovery potential?
- Opens a window of opportunities for precision electromagnetic physics at JLab

PRad-II: goals and how?



- Reduce the uncertainty of the r_p measurement by a factor of **3.8!**
- Reach an unprecedented low values of Q^2 : $4 \times 10^{-5} \text{ (GeV/c)}^2$
(**endorsed by the theory TAC report**)
- How?
 - Improving tracking capability by adding a second plane of tracking detector
 - Adding new rectangular cross shaped scintillator detectors to separate Moller from ep electrons in scattering angular range of 0.5^0 - 0.8^0
 - Upgrading HyCal
 - Replacing lead glass blocks by PbWO_4 modules (uniformity, resolutions, inelastic channel)
 - Converting to FADC based readout
 - Suppressing beamline background
 - Improving vacuum
 - Adding second beam halo blocker upstream of the tagger
 - Reducing statistical uncertainties by a factor of 4 compared with PRad
 - Three beam energies: 0.7, 1.4 and 2.1 GeV – ***0.7 GeV is critical to reach the lowest Q^2 ($4 \times 10^{-5} \text{ (GeV/c)}^2$)***
 - Improve radiative correction calculations by going to NNL order
 - Potential target improvement (***not used in projection***)

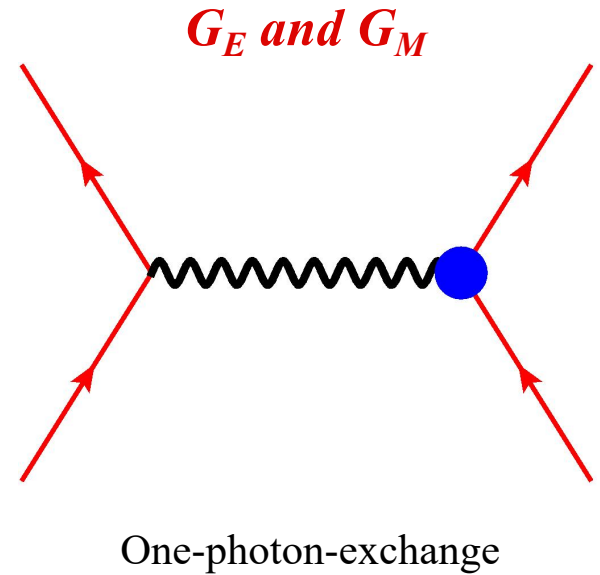
PRad-II Experimental Setup (Side View)



Electron-proton elastic scattering

Unpolarized elastic e-p cross section (*Rosenbluth separation*)

$$\begin{aligned} \frac{d\sigma}{d\Omega} &= \frac{\alpha^2 \cos^2 \frac{\theta}{2}}{4E^2 \sin^4 \frac{\theta}{2}} \frac{E'}{E} \left(\frac{G_E^p{}^2 + \tau G_M^p{}^2}{1 + \tau} + 2\tau G_M^p{}^2 \tan^2 \frac{\theta}{2} \right) \\ &= \sigma_M f_{rec}^{-1} \left(A + B \tan^2 \frac{\theta}{2} \right) \end{aligned}$$



$$Q^2 = 4EE' \sin^2 \frac{\theta}{2} \quad \tau = \frac{Q^2}{4M_p^2} \quad \epsilon = \left[1 + 2(1 + \tau) \tan^2 \frac{\theta}{2} \right]^{-1}$$

$$G_E^p(Q^2) = 1 - \frac{Q^2}{6} \langle r^2 \rangle + \frac{Q^4}{120} \langle r^4 \rangle + \dots$$

$$\langle r^2 \rangle = -6 \left. \frac{dG_E^p(Q^2)}{dQ^2} \right|_{Q^2=0}$$

At low Q^2 region such as PRad, the cross section is dominated by the G_E^2 term, G_M^2 effect included and systematic uncertainty assigned.

Extraction of ep Elastic Scattering Cross Section

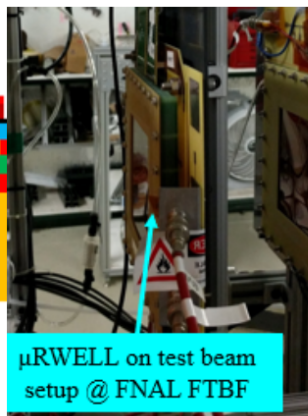
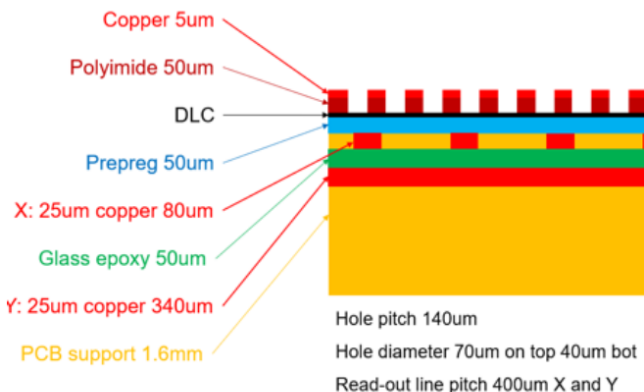
- To reduce the systematic uncertainty, the ep cross section is normalized to the Møller cross section:

$$\left(\frac{d\sigma}{d\Omega}\right)_{ep} = \left[\frac{N_{\text{exp}}(ep \rightarrow ep \text{ in } \theta_i \pm \Delta\theta_i)}{N_{\text{exp}}(ee \rightarrow ee)} \cdot \frac{\varepsilon_{\text{geom}}^{ee}}{\varepsilon_{\text{geom}}^{ep}} \cdot \frac{\varepsilon_{\text{det}}^{ee}}{\varepsilon_{\text{det}}^{ep}} \right] \left(\frac{d\sigma}{d\Omega}\right)_{ee}$$

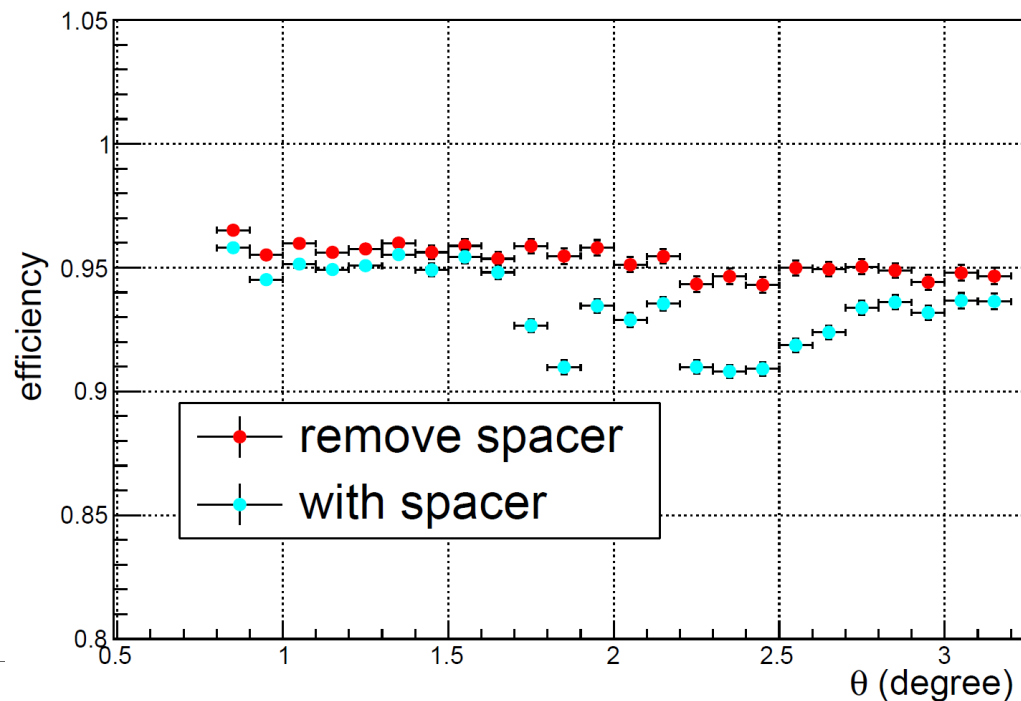
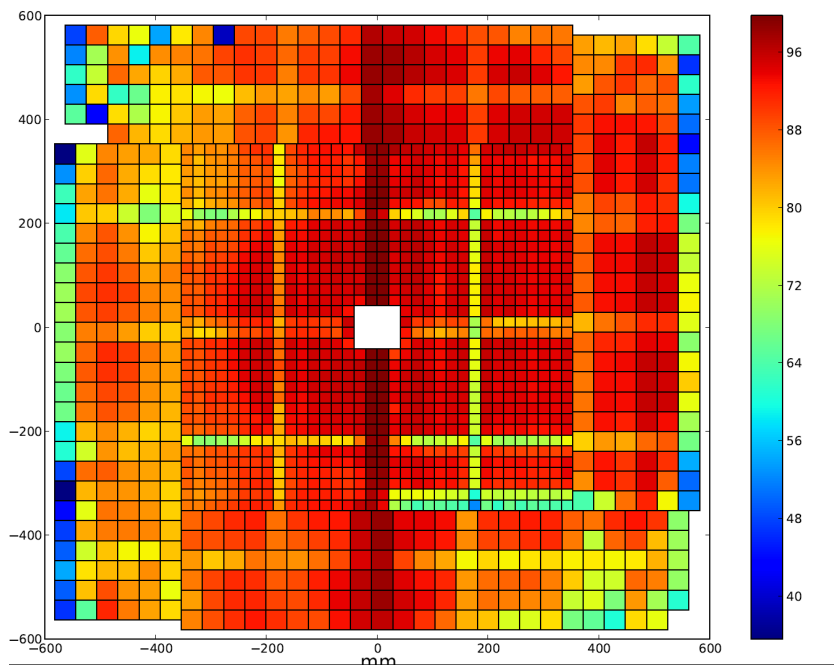
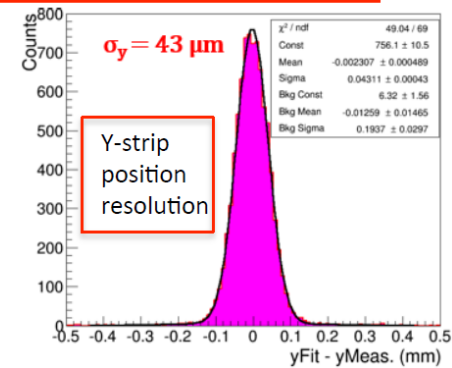
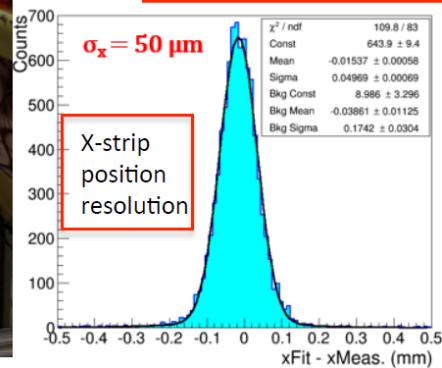
- Method 1: bin-by-bin method** – taking ep/ee counts from the same angular bin
 - Cancellation of energy independent part of the efficiency and acceptance
 - Limited coverage due to double-arm Møller acceptance
- Method 2: integrated Møller method** – integrate Møller in a fixed angular range and use it as common normalization for all angular bins
 - Needs to know the GEM efficiency well
- Luminosity cancelled from both methods
- PRad: Bin-by-bin range: 0.7° to 1.6° for 2.2 GeV, 0.75° to 3.0° for 1.1 GeV. Larger angles use integrated Møller method (3.0° to 7.0° for 1.1 GeV; 1.6° to 7.0° for 2.2 GeV)
- PRad-II: two planes of GEM/ μ Rwell allow for **integrated Møller method** for the entire experiment
- Event generators for unpolarized elastic ep and Møller scatterings have been developed based on complete calculations of radiative corrections – **PRad-II with NNL for RC**
 - A. V. Gramolin et al., J. Phys. G Nucl. Part. Phys. 41(2014)115001
 - I. Akushevich et al., Eur. Phys. J. A 51(2015)1 (beyond ultra relativistic approximation)
- A Geant4 simulation package is used to study the radiative effects, and an iterative procedure applied

$$\sigma_{ep}^{\text{Born}(exp)} = \left(\frac{\sigma_{ep}}{\sigma_{ee}}\right)^{\text{exp}} / \left(\frac{\sigma_{ep}}{\sigma_{ee}}\right)^{\text{sim}} \cdot \left(\frac{\sigma_{ep}}{\sigma_{ee}}\right)^{\text{Born}(model)} \cdot \sigma_{ee}^{\text{Born}(model)}$$

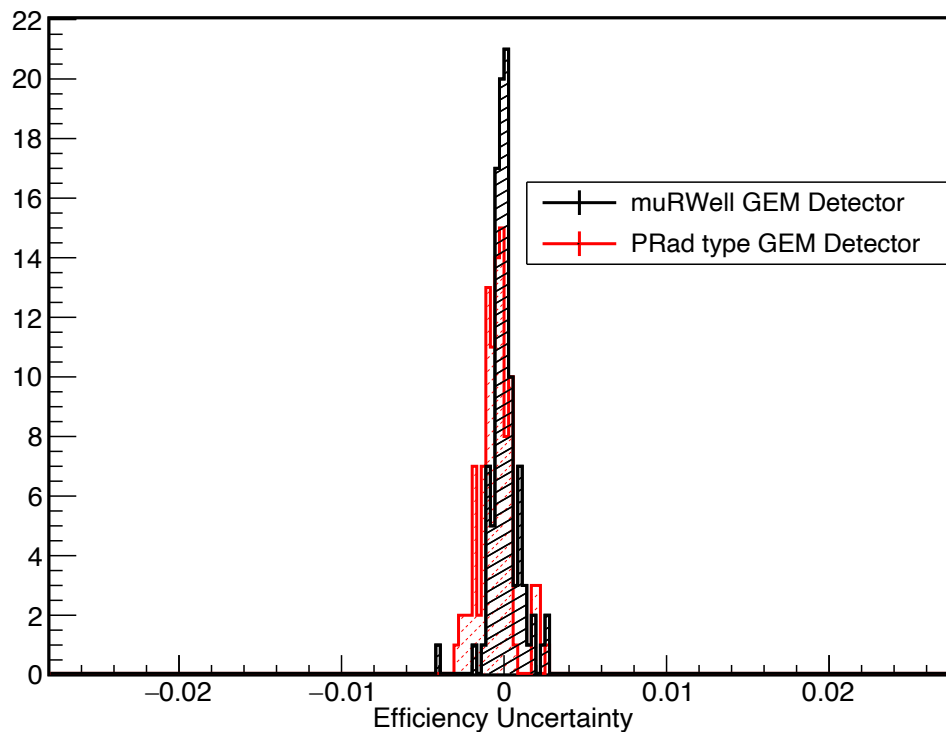
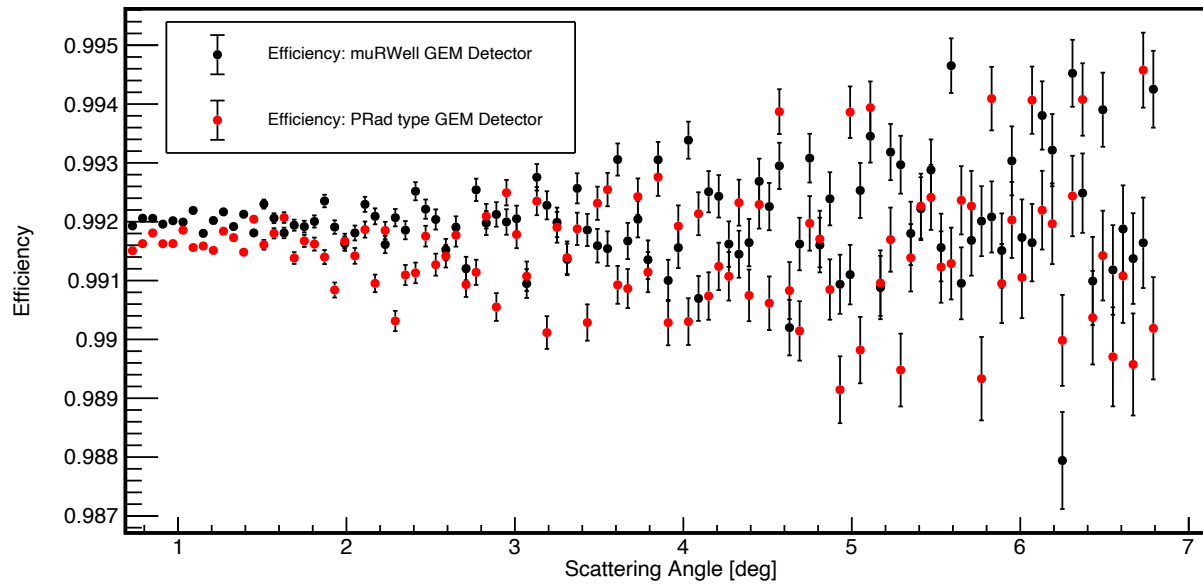
Latest development on tracking detector μ Rwell and improvements



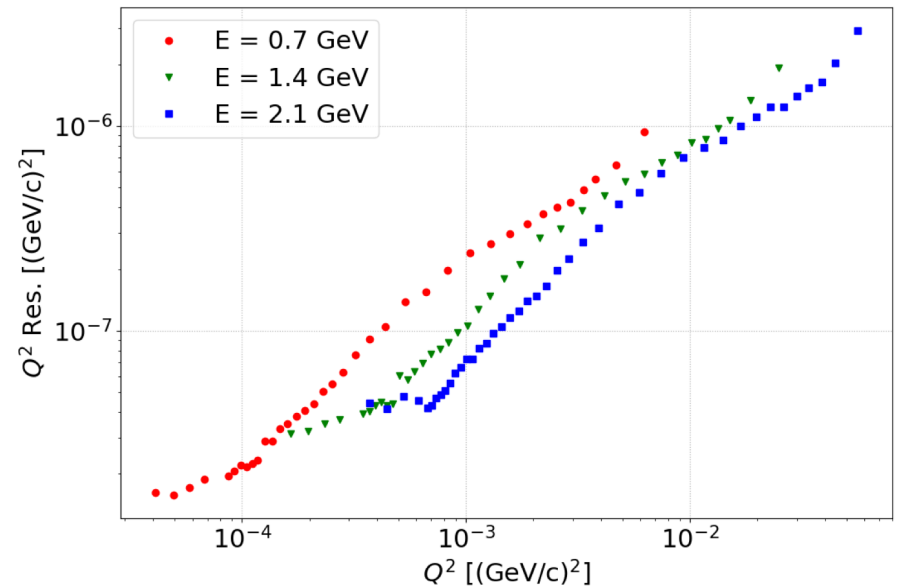
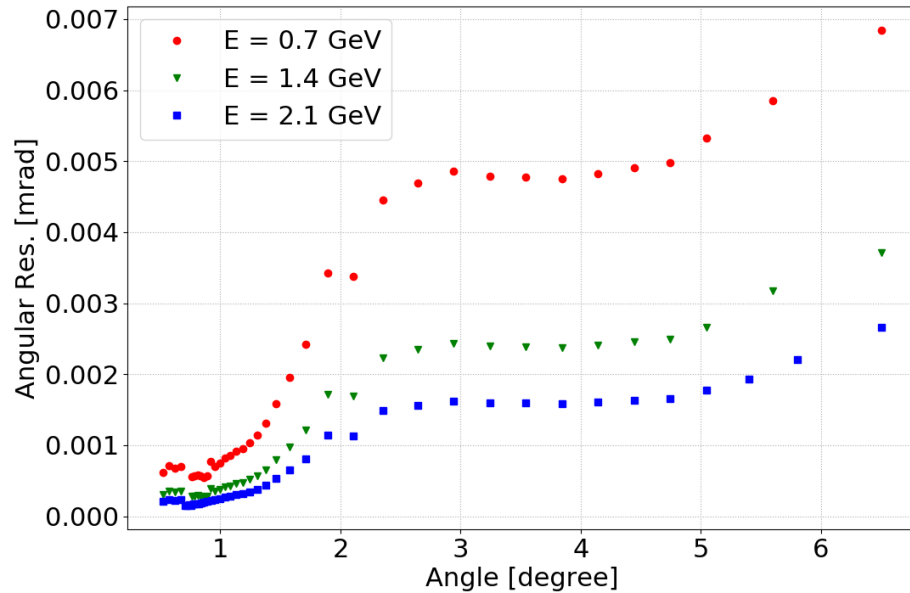
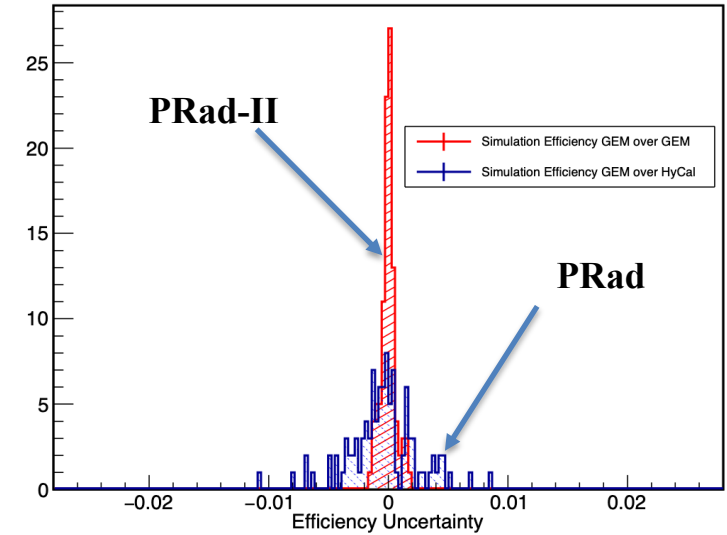
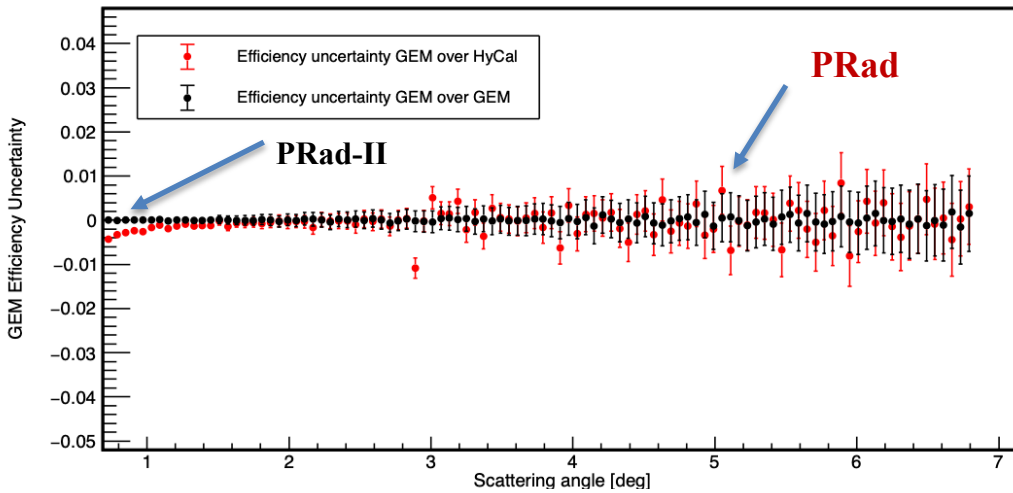
Preliminary μ Rwell results from Fermilab test beam



PRad-II: GEM versus μ RWELL

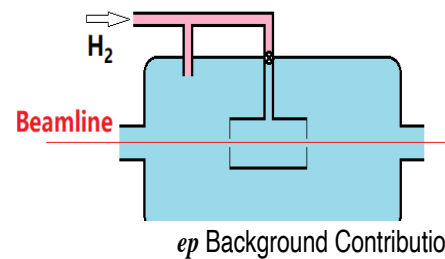
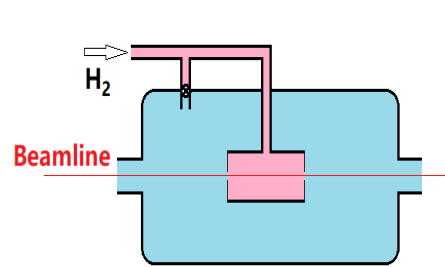


Improvements with the addition of a 2nd plane of GEMs/ μ RWELL

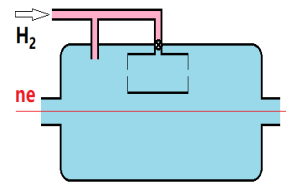
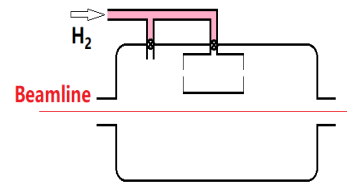
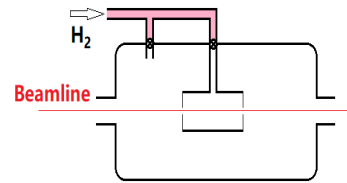


Background subtraction improvement with 2nd GEM/ μ RWELL

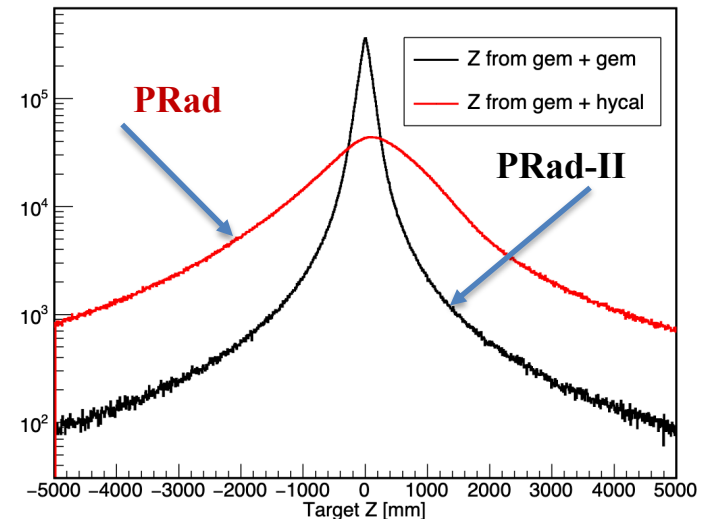
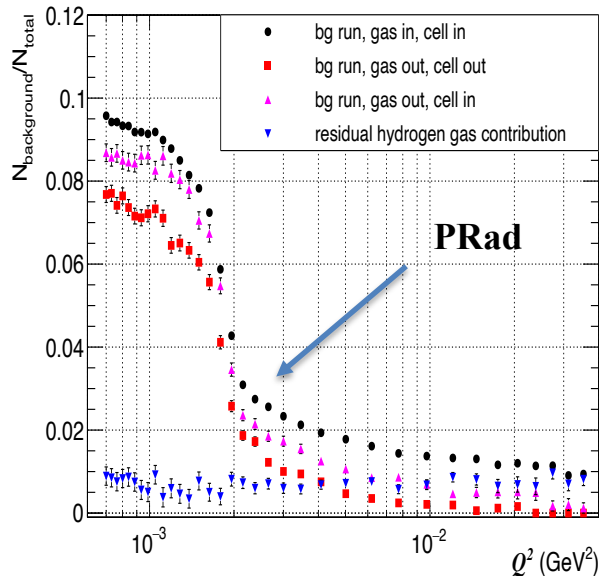
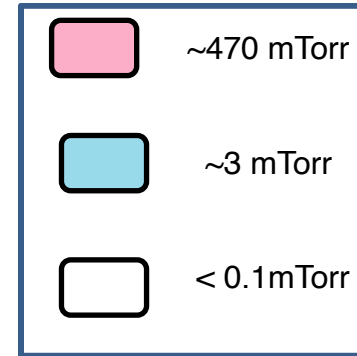
- Runs with different target conditions for background subtraction and systematic studies together with simulations (COMSOL finite element analysis)



ep Background Contribution

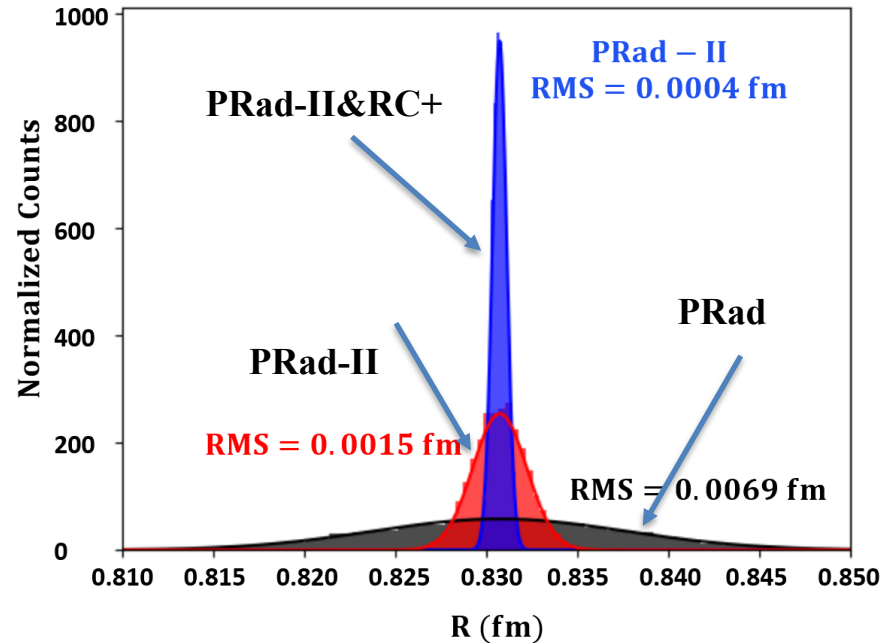
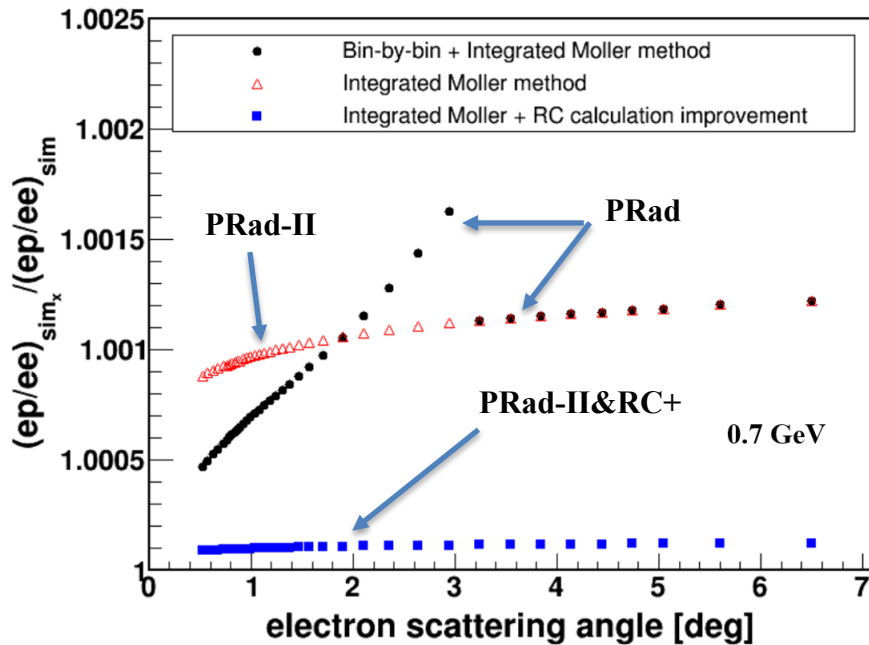


Pressure:



Improvement: addition of a 2nd plane of GEMs/ μ RWELL and RC calculations

- Improvement in GEM/ μ Rwell efficiency determination allows for integrated Møller method
- Major improvement in radius determination associated with integrated Møller
- More improvement expected with the RC calculations at the NNL -- RC+

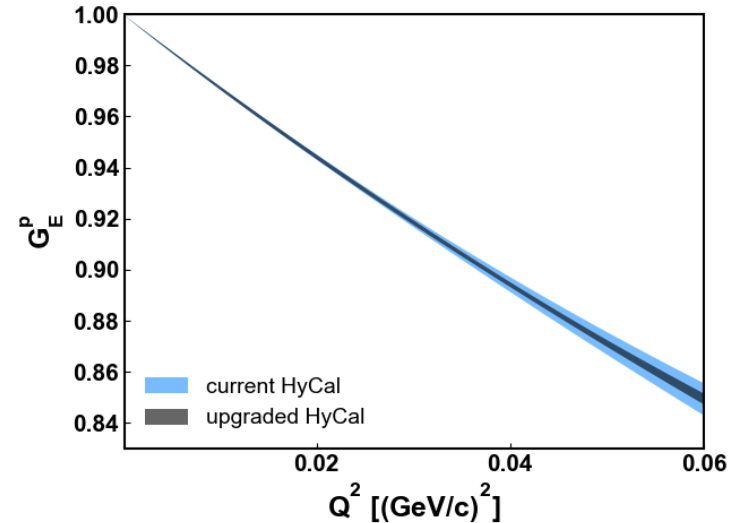
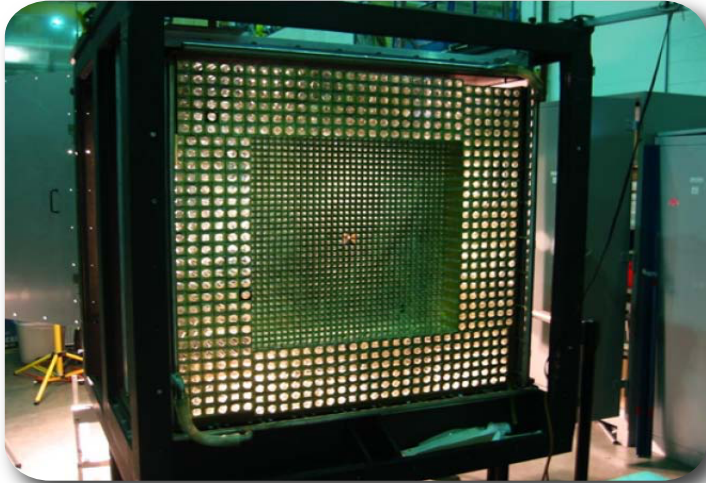


Bin-by-bin + Integrated Møller Method (PRad method):

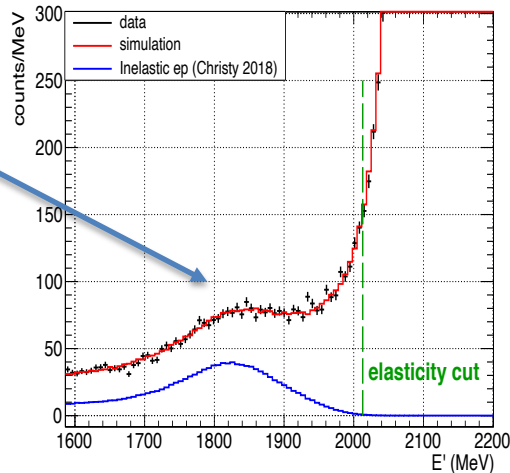
- Bin-by-bin method is applied below 3.0 deg at 0.7, 1.4 GeV and 1.6 deg at 2.1 GeV
- Integrated Møller method applied in the other angular bins

Improvements to HyCal

- HyCal: inner 1156 PWO_4 modules with outer 576 lead glass modules originally funded by NSF-MRI for the PrimEX experiment (*Science* 6490, 506-509 (2020))
- Replacing all lead-glass by PbWO_4 leads to
 - Better uniformity, better position and energy resolutions
 - major improvement suppressing inelastic contamination – more important at higher Q^2
- Convert to FADC based readout allowing data taking rate increase by a factor of 7 compared to PRad

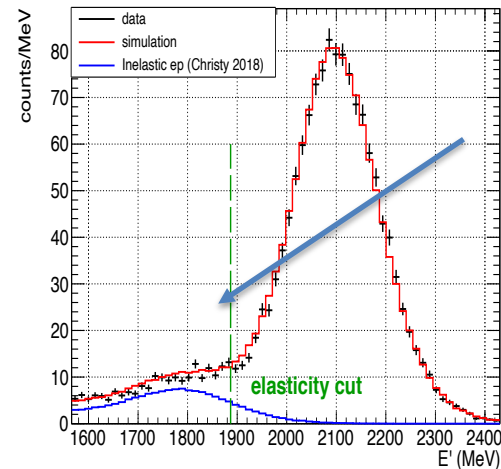


spectrum for $3.0^\circ < \theta < 3.3^\circ$ ($Q^2 \sim 0.014 \text{ GeV}^2$)



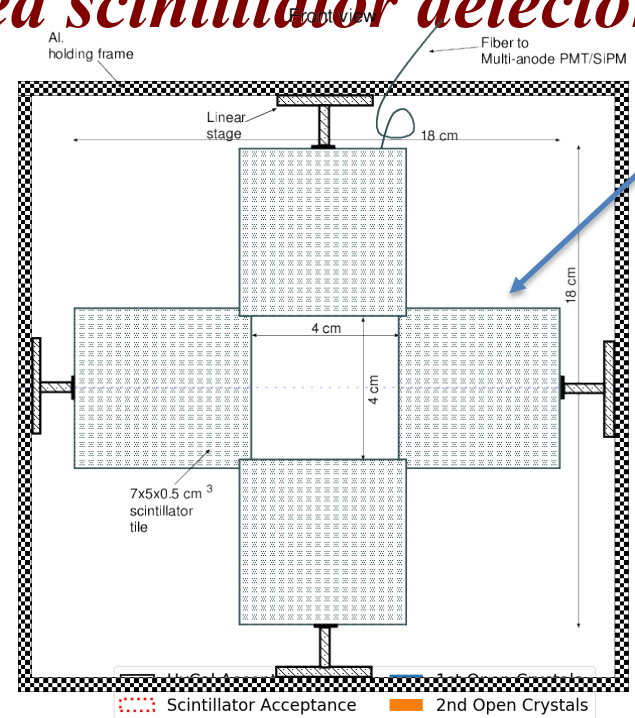
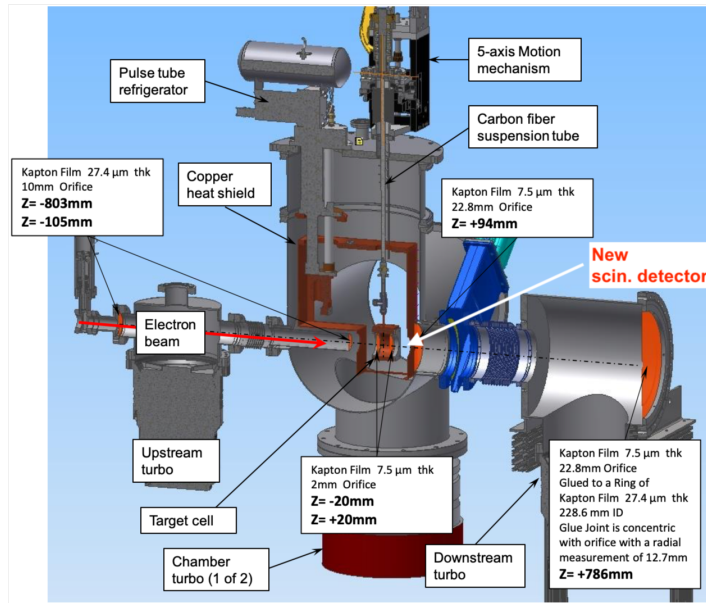
PbWO_4 region

spectrum for $6.0^\circ < \theta < 7.0^\circ$ ($Q^2 \sim 0.059 \text{ GeV}^2$)



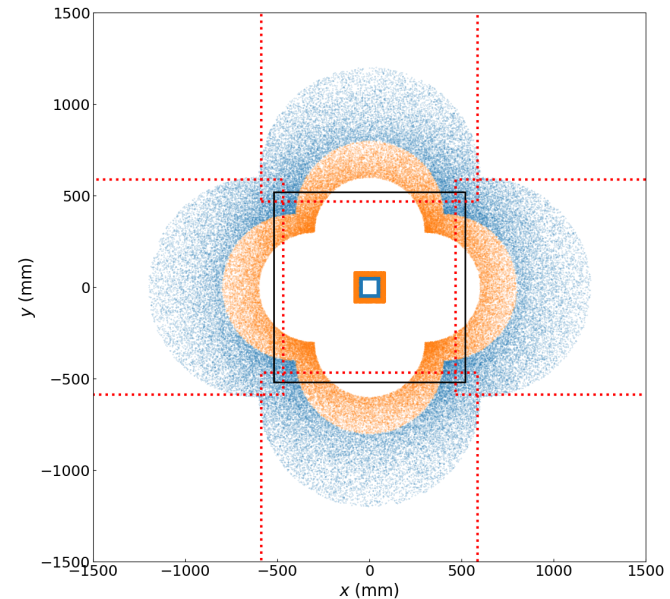
Lead glass region

New rectangular cross shaped scintillator detectors

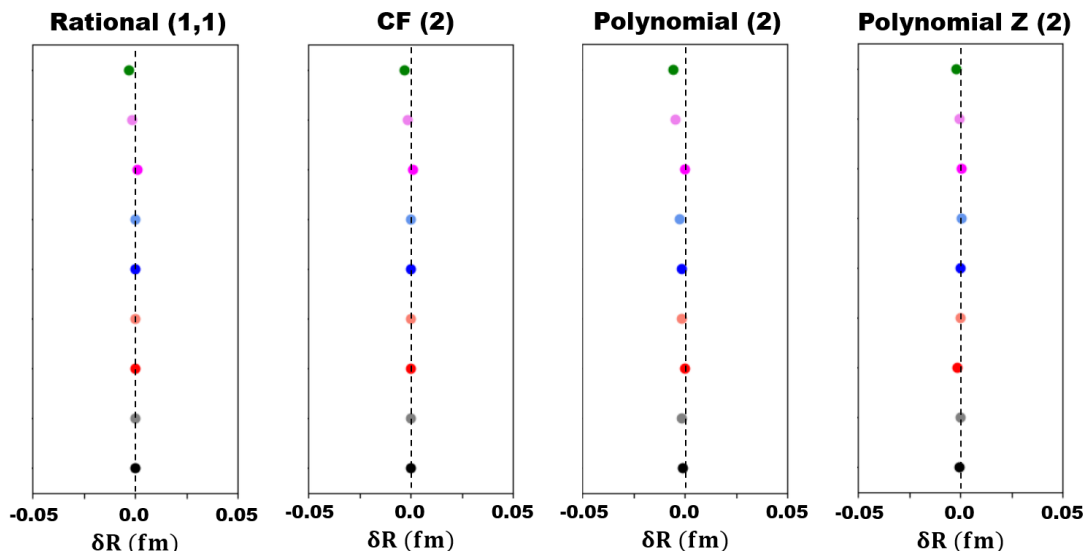


Not to scale

- Four 7x5x0.5 cm³ tiles of plastic scintillators
- Arranged in a cross shape with a 4x4 cm² hole in the center
- Each tile is attached to a linear stage in x-y plane
- Each tile is read out using optical fibers and multi-anode PMTs or SiPMs

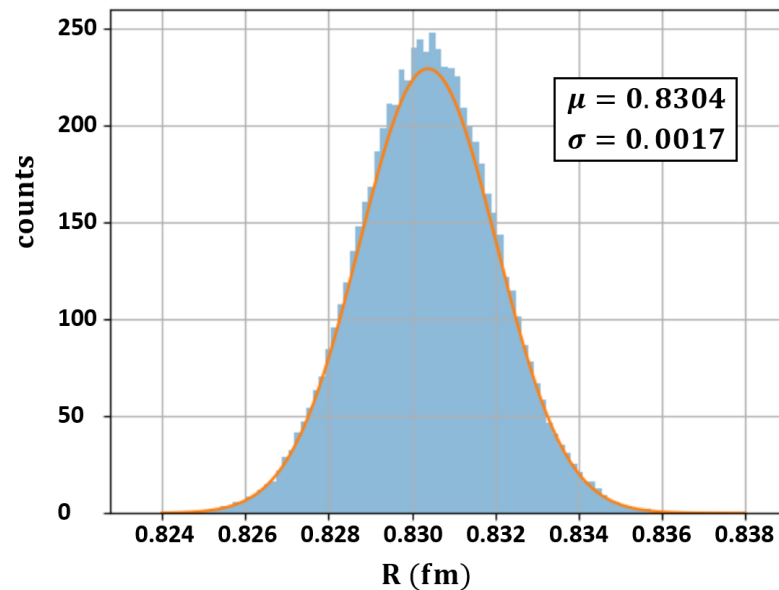
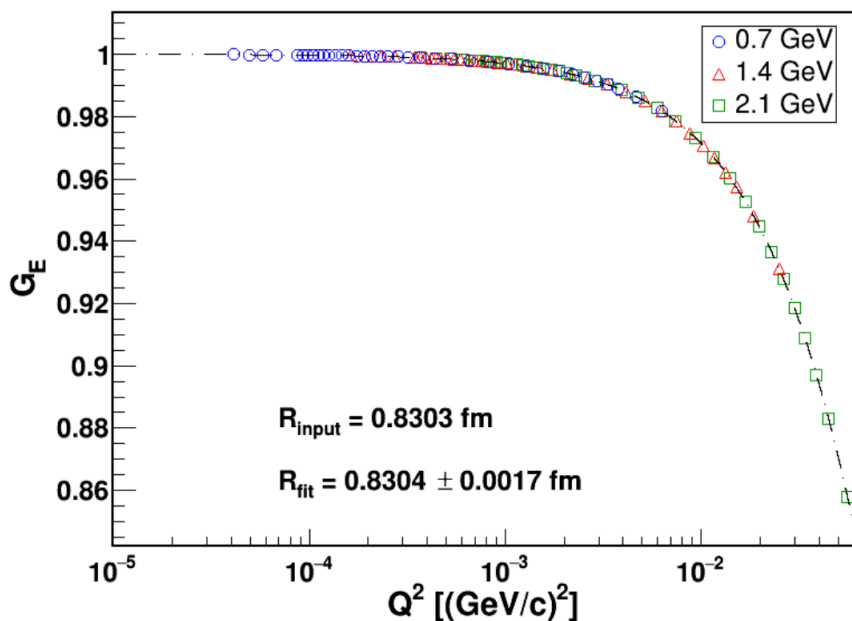


Robustness fitting study for PRad-II carried out



Ye-2018
 Bernauer-2014
 Alarcón-2017
 Arrington-2007
 Arrington-2004
 Kelly-2004
 Gaussian
 Monopole
 Dipole

X. Yan *et al.*
 PRC98, 025204 (2018))



Input: The PRad data fitted to the 2nd order polynomial z expansion then used to generate pseudo-data for PRad-II
Output: The pseudo-data then fitted to Rational(1,1) with three floating normalization parameters

Beam requirements and request

Energy (GeV)	current (nA)	polarization (%)	size (mm)	position stability (mm)	beam halo
0.7	20	Non	<0.1	≤ 0.1	$\sim 10^{-7}$
1.4	70	Non	<0.1	≤ 0.1	$\sim 10^{-7}$
2.1	70	Non	<0.1	≤ 0.1	$\sim 10^{-7}$

	Time [day]
Setup checkout, tests and calibration	7
Production at 0.7 GeV	4
Production at 1.4 GeV	5
Production at 2.1 GeV	15
Empty target runs	8
Energy change	1
Total	40

We have addressed the TAC questions and provided answers to the PAC

Improvement of PRad-II over PRad

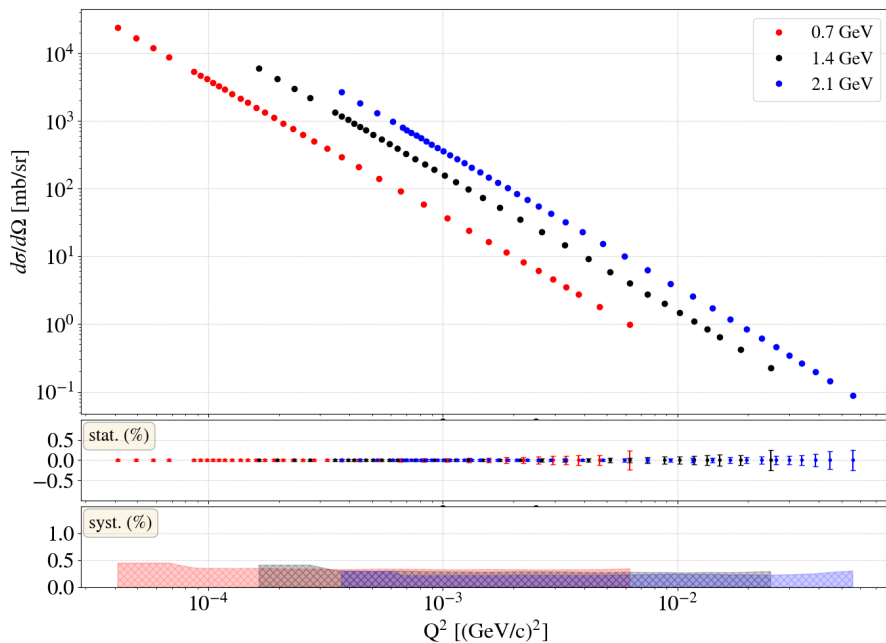
Item	PRad δr_p [fm]	PRad-II δr_p [fm]	Result of
Stat. uncertainty	0.0075	0.0017	more beam time
GEM efficiency	0.0042	0.0008	2nd tracking detector
Acceptance	0.0026	0.0002	2nd tracking detector
Beam energy related	0.0022	0.0002	2nd tracking detector
Event selection	0.0070	0.0027	2nd tracking + HyCal upgrade
HyCal response	0.0029	negligible	HyCal upgrade
Beam background	0.0039	0.0016	better vacuum 2nd halo blocker vertex res. (2nd tracking)
Radiative correction	0.0069	0.0004	improved calc.
Inelastic ep	0.0009	negligible	Upgraded HyCal
G_M^p parameterization	0.0006	0.0005	-
Total syst. uncertainty	0.0115	0.0032	
Total uncertainty	0.0137	0.0036	



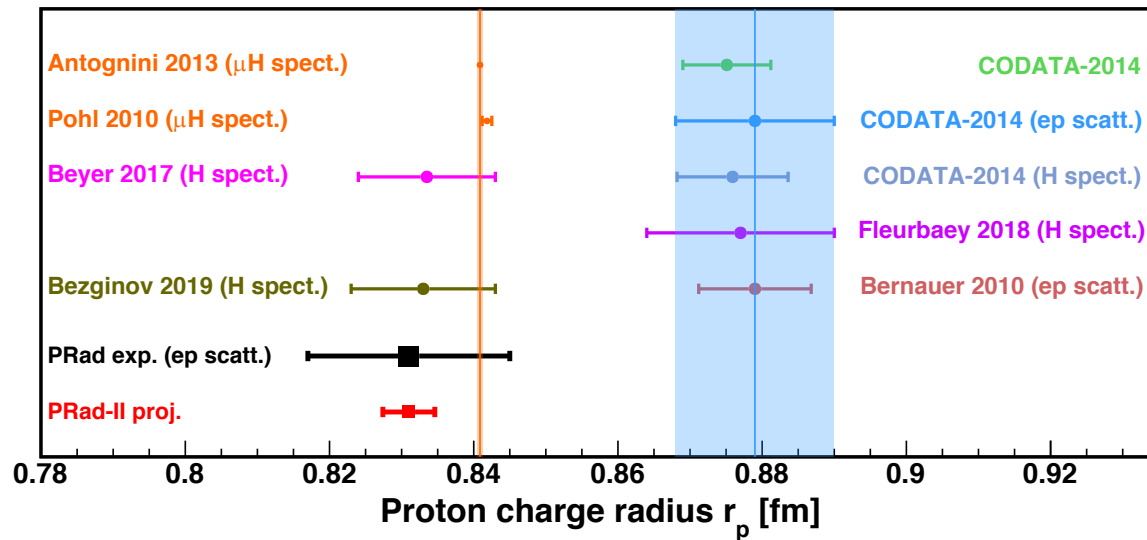
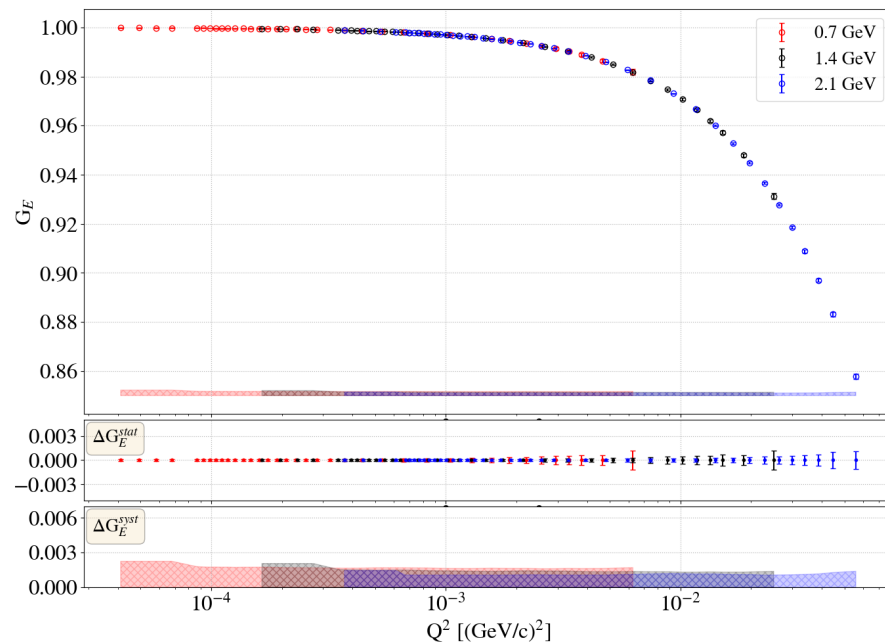
A factor of 3.8 improvement!

Projections for PRad-II

Differential Cross section



Electric form factor



Summary and outlook

- The PRad experiment demonstrated the power of calorimetric method for the proton radius measurement, and reported high-impact result on r_p
- The PRad-II will push for the precision of such method and improve the r_p measurement by a factor **3.8!**
- High precision data from PRad-II on G_E^p will help resolve the differences between PRad and modern ep experiments including A1@Mainz
- High precision result on r_p from PRad-II will allow for systematic study between results from ep and muonic hydrogen measurements
- PRad-II may open a new window of opportunities for precision electromagnetic physics

Acknowledgement: The PRad collaboration

supported in part by NSF MRI PHY-1229153 and the U.S. Department of Energy under contract number DE-FG02-03ER41231